Mutations in *BRAF* and *KRAS* Differentially Distinguish Serrated versus Non-Serrated Hyperplastic Aberrant Crypt Foci in Humans

Daniel W. Rosenberg,[1,2] Shi Yang,[5] Devon C. Pleau,[1,2] Emily J. Greenspan,[2] Richard G. Stevens,[1,3] Thiruchandurai V. Rajan,[1,4] Christopher D. Heinen,[1,2] Joel Levine,[1] Yijian Zhou,[2] and Michael J. O'Brien[5]

[1]Colon Cancer Prevention Program, NEAG Comprehensive Cancer Center; [2]Center for Molecular Medicine; Departments of [3]Community Medicine and [4]Immunology, UCHC Department of Pathology and Laboratory Medicine, University of Connecticut Health Center, Farmington, Connecticut; and [5]Boston University School of Medicine, Boston, Massachusetts

Abstract

We previously reported that colon carcinomas, adenomas, and hyperplastic polyps exhibiting a serrated histology were very likely to possess *BRAF* mutations, whereas when these same advanced colonic lesions exhibited non-serrated histology, they were wild type for *BRAF*; among hyperplastic polyps, *KRAS* mutations were found mainly in a non-serrated variant. On this basis, we predicted that hyperplastic aberrant crypt foci (ACF), a putative precancerous lesion found in the colon, exhibiting a serrated phenotype would also harbor *BRAF* mutations and that non-serrated ACF would not. In contrast, *KRAS* mutations would be found more often in the non-serrated ACF. We examined 55 ACF collected during screening colonoscopy from a total of 28 patients. Following laser capture microdissection, DNA was isolated, and mutations in *BRAF* and *KRAS* were determined by direct PCR sequencing. When hyperplastic lesions were further classified into serrated and non-serrated histologies, there was a strong inverse relationship between *BRAF* and *KRAS* mutations: a $BRAF^{V600E}$ mutation was identified in 10 of 16 serrated compared with 1 of 33 non-serrated lesions ($P = 0.001$); conversely, *KRAS* mutations were present in 3 of 16 serrated compared with 14 of 33 non-serrated lesions. Our finding of a strong association between *BRAF* mutations and serrated histology in hyperplastic ACF supports the idea that these lesions are an early, sentinel, or a potentially initiating step on the serrated pathway to colorectal carcinoma. [Cancer Res 2007;67(8):3551–4]

Introduction

Aberrant crypt foci (ACF) are microscopic mucosal abnormalities, a subset of which may be precursors to advanced colonic neoplasms (1–3). The traditional pathway to colorectal cancer (adenoma-carcinoma sequence) is supported by a great deal of evidence (4). More recently, an alternative pathway has been proposed based on the progression of colonic lesions with a serrated morphology (5–7). A recent finding in the serrated pathway is that *BRAF* mutations were strongly associated with serrated histologic subtypes of hyperplastic polyps and adenomas (8) and rare or absent in non-serrated lesions (9). In addition, whereas *KRAS* mutations are found in advanced adenomas of both pathways, among hyperplastic polyps, they were largely restricted to a non-serrated variant (10). Based on these observations, we predicted that those hyperplastic ACF that show serrated histology would be much more likely to exhibit *BRAF* mutations than non-serrated ACF, and that *KRAS* would show an opposite relationship. Histologic criteria for distinction between a serrated and non-serrated phenotype have been described for hyperplastic polyps (10, 11); we applied the same criteria to evaluate hyperplastic ACF in the present study.

Materials and Methods

Subject selection. Twenty-eight patients underwent total colonoscopy at the John Dempsey Hospital (JDH) at the University of Connecticut Health Center (UCHC) in accordance with Institutional policies. Patients suspected of having familial adenomatous polyposis or hereditary non-polyposis colorectal cancer were excluded from this study. This study was done after approval by an Institutional Review Board, and all subjects provided written informed consent.

ACF collection and characterization. ACF were isolated from grossly normal-appearing colonic mucosa by biopsy *in situ* during the high-resolution, close-focus chromoendoscopy portion of the total colonoscopy procedure. The distal 20 cm of colon and rectum was examined after washing with 10 to 20 mL of 20% *N*-acetylcysteine followed by water to remove the surface mucin. ACF were visualized and photographed using an Olympus close-focus colonoscope (XCF-Q160ALE; Olympus Corp., Center Valley, PA) that by employing a focal length of 2 to 100 mm permits high magnification (×60) to be sustained over a longer visualizing distance. This allows for an increased ACF retrieval rate on biopsy (12, 13).

Representative frozen sections of ACF were stained with H&E for routine histologic analysis by light microscopy of coded specimens by M.J.O, a GI pathologist who was blinded to the clinical and molecular findings. Dysplastic ACF were characterized histologically by enlarged upper crypt regions of irregular shape with stratified, elongated nuclei and dysplastic appearance. Hyperplastic ACF were further characterized using criteria that have been applied to hyperplastic polyps (10). Serrated hyperplastic ACF were defined as those that showed crypts with a stellate luminal shape (serrated on oblique or cross-section) and a prominent component of columnar cells with microvesicular cytoplasm. Non-serrated hyperplastic ACF lacked crypt serration, whereas goblet cells were prominent, and in longitudinal or oblique sections, tufting of the surface epithelium was frequently evident.

Laser capture microdissection and DNA extraction. Frozen serial sections of ACF were prepared at 5 to 7 μm thickness on glass slides. Laser capture microdissection was done on frozen sections using the Veritas microdissection instrument (Molecular Devices, Sunnyvale, CA) as described in our previous studies (12, 13). Whenever possible, adjacent normal mucosal cells directly abutting the aberrant crypts were collected separately by laser capture. On average, 1,500 to 3,000 cells were collected from each sample, and DNA was extracted using the Picopure DNA extraction kit (Molecular Devices).

Mutation analyses for $BRAF^{(V600E)}$ and *KRAS* codon 12/13. Mutation analyses for $BRAF^{(V600E)}$ and KRAS codon 12/13 were done on DNA samples

Requests for reprints: Daniel W. Rosenberg, University of Connecticut Health Center, 263 Farmington Avenue, Farmington, CT 06030-3101. Phone: 860-679-8704; Fax: 860-679-1151; E-mail: Rosenberg@nso2.uchc.edu.

doi:10.1158/0008-5472.CAN-07-0343

as described in our previous studies (8, 10). Briefly, DNA (25 ng) samples were extracted from microdissected colorectal ACF tissues. A 189-bp fragment of the *BRAF* gene spanning codon 600 was amplified using the following primers: F, 5′-CCTAAACTCTTCATAATGCTTGCTC-3′ and R, 5′-CCACAAAATGGATCCAGACA-3′. After gel electrophoresis to confirm the amplified product, the PCR product was enzymatically cleaned with 2 μL of EXO SAP-IT (U.S. Biochemical Corp., Cleveland, OH). A 2.5-μL aliquot of the product was sequenced using the forward primer with an ABI BigDye TerV3.1 Cycle Sequencing kit on an ABI 9700 thermocycler (Applied Biosystems, Inc., Foster City, CA). Fifteen microliters of ethanol-precipitated reaction product was sequenced by capillary electrophoresis with a 3100-avant Genetic Analyzer (Applied Biosystems). The data were analyzed using ABI DNA Sequencing Analysis Software 3.7. A positive control (sample with a known mutation at codon 600 from a human colon carcinoma) and a negative control (placental DNA; Sigma, St. Louis, MO) were included in each sequencing analysis.

Similarly, *KRAS* codon 12 and 13 mutations were also analyzed from an amplified 205-bp fragment that spanned codons 12 and 13 using the following primers: forward, 5′-GTACTGGTGGAGTATTTGAT-3′ and reverse, 5′-TCTATTGTTGGATCATATTC-3′. The forward primer was used for the sequencing reaction. DNA with a mutation at codon 12 (SW480 cells) and a negative control (placental DNA; Sigma) were included in each sequencing analysis.

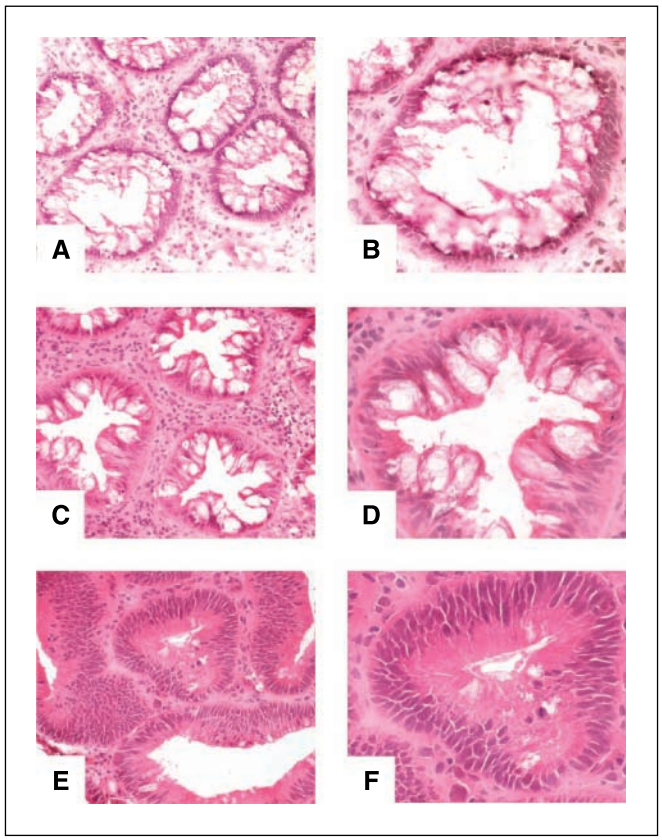

Figure 1. Histology of ACF. H&E-stained frozen sections of the three categories of ACF: non-serrated hyperplastic (*A* and *B*), serrated hyperplastic (*C* and *D*), and dysplastic (*E* and *F*). *A,* cross-section through an enlarged circular or oval upper crypt of a KRAS-mutated, non-serrated hyperplastic ACF that exhibit numerous goblet cells (*B*, detail). *C,* cross-section through a BRAF-mutated, serrated ACF that shows an enlarged crypt with a stellate lumen (serrated on longitudinal section). *D,* detail of the component epithelial cells of the serrated ACF to consist of a mixture of goblet cells and columnar cells that have a microvesicular cytoplasm. *E* and *F,* section through the upper crypts of a dysplastic ACF to show enlarged irregularly shaped crypts that are lined by cells with mucus-depleted cytoplasm and nuclei that are stratified, elongated, and dysplastic in appearance.

Table 1. Mutation frequency in hyperplastic and dysplastic ACF

Genetic aberration	Hyperplastic ACF		Dysplastic ACF
	Non-serrated	Serrated	
BRAF*	1/33 (3%)*	10/16 (62.5%)*	0/6 (0%)
KRAS †	14/33 (42%) †	3/16 (18.75%) †	1/6 (16.6%)

*$P = 0.001$ (χ^2).
†$P = 0.2$.

***APC* mutation status and β-catenin immunofluorescence.** For *APC* sequencing, DNA was extracted from microdissected tissue and amplified using four overlapping primer sets within exon 15 that encompasses the mutation cluster region (MCR) using a previously described method (14). To eliminate the possibility of a germ-line mutation, stroma adjacent to the ACF as well as a second ACF and adjacent stroma from the same patient was sequenced. CaCo-2 cells were used as a positive control, and HCT-116 cells were used as a negative control for the presence of an *APC* mutation.

Frozen sections (7 μm) were prepared and fixed in 10% neutral buffered formalin solution, dehydrated through graded ethanol, washed in xylene, and paraffinized at 58°C. Following antigen retrieval by heating in 0.01 mol/L sodium citrate buffer (pH 6.0), sections were incubated in a blocking solution of 10% normal goat serum in 10% PBS (pH 7.4) for 30 min to prevent nonspecific binding. Sections were incubated overnight at 4°C in a humidified chamber with mouse monoclonal anti-β-catenin antibody (IgG1 isotype; Sigma) diluted 1:2,000 in blocking solution. Slides were washed in 10% PBS and incubated in goat anti-mouse fluorescence antibody (Alexa Fluor 488; Molecular Probes, Carlsbad, CA) for 30 min in a humidified chamber protected from light. After washing in PBS, slides were stained with 4′,6-diamidino-2-phenylindole diluted in 1:2,000 10% PBS for 1 min and washed in 10% PBS twice. Sections were mounted in Vectashield mounting medium for fluorescence (Vector Laboratories, Burlingame, CA).

Microsatellite instability. For microsatellite instability (MSI) analysis, DNA was isolated from microdissected ACF and matched adjacent normal colon epithelia, and MSI status was determined using the National Cancer Institute–recommended panel of five microsatellite markers (BAT25, BAT26, D2S123, D5S346, and D17S250) as previously conducted in our laboratory (15). An ACF was considered to be MSI-H if two or more markers showed instability; MSI-L if one marker showed instability; and MSS if no markers show instability when compared with matched normal DNA. Two observers (E.G. and C.H.) did the evaluation of MSI independently, and the results were reported without knowledge of patient history or *hMLH1* or *MGMT* MSP status. Any questionable or inconclusive assays were repeated at least once before making a determination.

Statistical analysis. For comparison of *KRAS, BRAF*, and *APC* mutations, analysis was carried out for two-sided *P* values using the χ^2 test and the web χ^2 calculator.[6]

Results

Identification of ACF. ACF were identified in the distal 20 cm in 28 patients during screening colonoscopy procedures done at the JDH. The mean ± SD number of ACF observed in this study was 9.8 ± 6.2 per patient. Anywhere from 2 to 12 biopsy

[6] http://www.georgetown.edu/faculty/ballc/webtools/web_chi.html

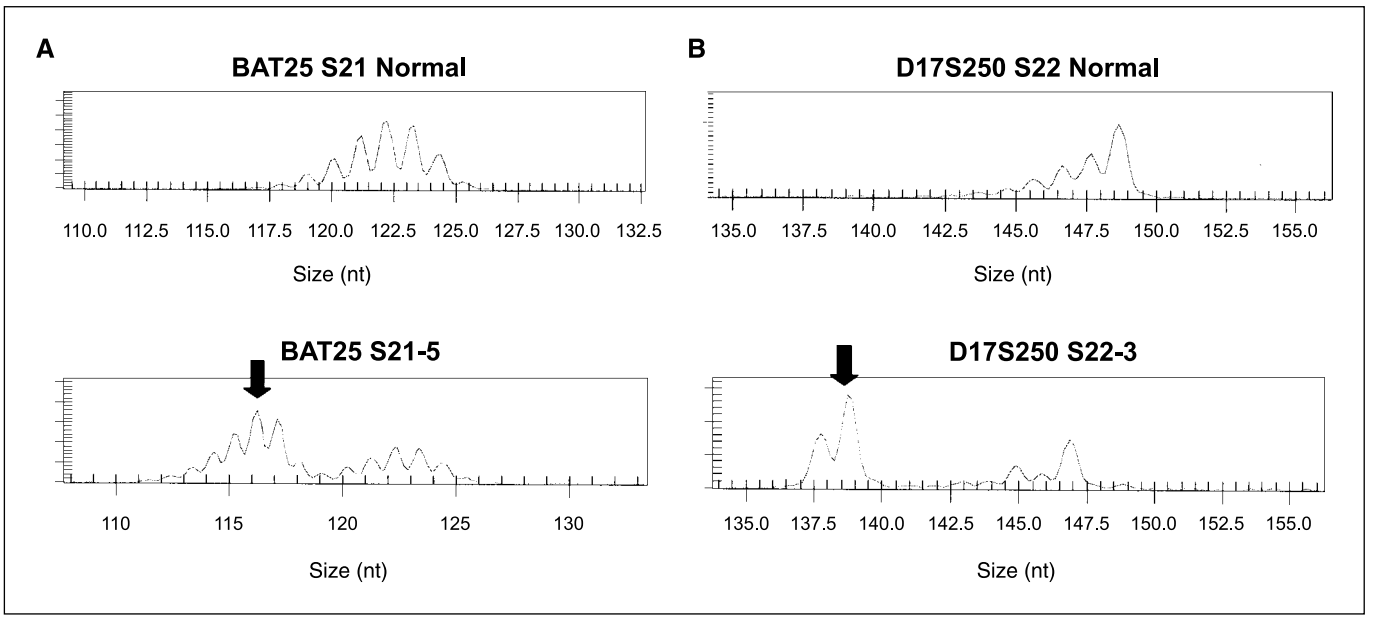

Figure 2. Representative examples of MSI in laser-captured hyperplastic ACF. *A,* example of MSI detected at the BAT25 marker. ACF S21-5 has a novel allele (~116 nucleotides). *B,* example of MSI detected at the D17S250 marker. ACF S22-3 has a novel allele (~139 nucleotides).

specimens were removed from each patient (mean = 5.12). A total of 55 ACF were randomly selected for inclusion in this study. The histology of the ACF biopsies was determined in H&E-stained sections. Figure 1 shows representative histology of a serrated and non-serrated hyperplastic variants and dysplastic ACF on cross-sections of the upper crypts. Of the 55 ACF that were included in the study group, 49 of 55 (89%) were classified as hyperplastic, whereas 6 of 55 (10.9%) were classified as dysplastic (microadenomas).

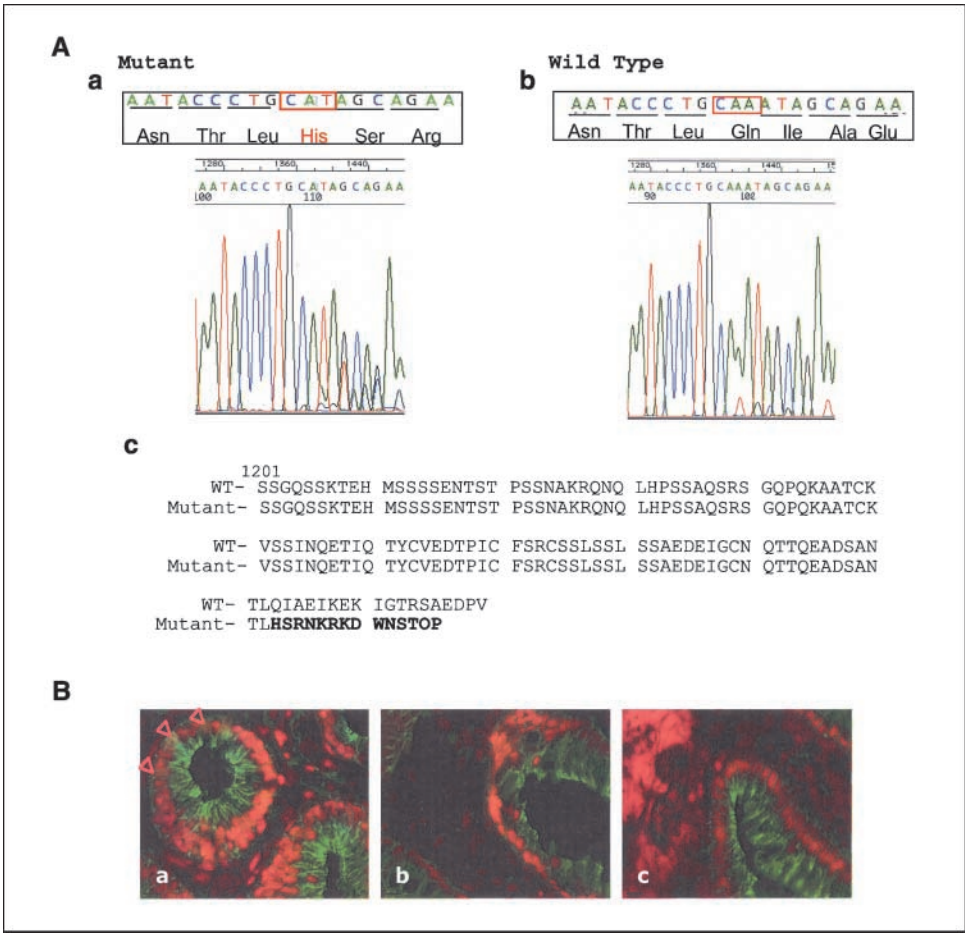

Figure 3. *A, a,* novel *APC* mutation. *APC* sequencing results from ACF with a mutation at codon 1303 (deletion of AA resulting in a Q1303H mutation.) *b, APC* sequencing results representing the wild-type sequence from adjacent stroma to the ACF with the mutation. Analysis of a second ACF (S6-2) and adjacent stroma from the same patient also displayed wild-type *APC* confirming the mutation is somatic. *c,* comparison of wild-type (*WT*) and mutant APC protein sequence from codon 1201 to 1320. The Q1303H mutation results in the truncation of the APC protein at codon 1313. *B,* immunofluorescence analysis of β-catenin in ACF. Merged immunofluorescence images using Alexa Fluor 488–labeled β-catenin (*green*) and 4′,6-diaminido-2-phenylindole–stained nuclei (*red*) as described in Materials and Methods. *a,* a serrated microadenoma with a truncation mutation (AA deletion at codon 1303) in the *APC* gene. β-Catenin staining was readily apparent in the cell membranes, indicated by the merged image (*yellow*). Staining was also found within a subset of nuclei within the adenoma (indicated by the arrowheads). *b,* a dysplastic ACF with wild-type APC, showing only membrane expression of β-catenin. *c,* a representative hyperplastic ACF showing only membrane associated β-catenin staining.

***BRAF* and *KRAS* mutations and MSI.** Table 1 shows the distribution of *BRAF* and *KRAS* mutations in serrated and non-serrated hyperplastic ACF and dysplastic ACF. We tested the a priori hypothesis that *BRAF* mutations would be associated with serrated lesions. Results were consistent with our prediction ($P = 0.001$). In addition, *KRAS* mutations were more common in the non-serrated than serrated lesions, although not significantly so. None of the 55 ACF had both *BRAF* and *KRAS* mutations.

The proportion of ACF that were positive for MSI-H was 11% in hyperplastic (5 of 45) and 25% (1 of 4) in dysplastic ACF. Although >70% of MSI carcinomas exhibit *BRAF* mutations, MSI was not associated with *BRAF* mutations in ACF, supporting previously reported studies that MSI is a late event in the serrated polyp pathway to sporadic carcinogenesis (9, 16). The rarity of MSI in both serrated and non-serrated advanced sporadic adenomas suggests that MSI-H ACF are self-limited. Several representative examples of MSI in ACF are shown in Fig. 2.

***APC* mutation status and β-catenin immunofluoresence.** The MCR, located within exon 15, encompasses ~90% of *APC* mutations reported in both familial and sporadic colorectal cancers (17); thus, amplification was done on this region. Forty ACF were sequenced for *APC* mutations within the MCR. As shown in Fig. 3*A*, we found a novel *APC* mutation, a deletion of two adenine bases at codon 1303, in one of six dysplastic ACF. No mutations were found in the 34 hyperplastic ACF examined.

To determine whether the *APC* mutation may result in a functional alteration, immunofluorescence for β-catenin was done on serial sections. As shown in Fig. 3*B*, the dysplastic ACF with a confirmed *APC* mutation (*a*) shows both membrane-associated as well as nuclear staining for β-catenin (*arrows*). A second dysplastic ACF showed no evidence of nuclear β-catenin staining (*b*). In Fig. 3*B* (*c*) is a hyperplastic ACF showing prominent membrane-associated staining of β-catenin with no nuclear staining evident.

Discussion

There is interest in whether ACF, or a subset of them, are premalignant or on the path to a more advanced neoplastic lesion in the colon. The traditional pathway posits an adenoma-carcinoma sequence, with dysplastic ACF as the earliest identifiable lesion (4). Dysregulation of Wnt signaling, typically through *APC* mutations, is the distinguishing feature of this pathway, which accounts for upwards of two thirds of all colorectal cancer (4). However, dysplastic ACF are uncommon, whereas hyperplastic ACF are much more prevalent. These latter hyperplastic lesions have been observed in almost all persons over age 50, with an average frequency in the distal colorectum of about 5 to 10 (18). The question is whether hyperplastic ACF can be informative about future risk of colorectal cancer. In a recent study, Beach et al. (19) reported a very low frequency (4%, 3 of 26) of *BRAF* mutations in a sample of "heteroplastic" ACF that were not classified further. A notably high frequency of *KRAS* mutations (46%) in the samples in this report suggests that non-serrated ACF may have been overrepresented (20). The prevalence of advanced *BRAF*-mutated, serrated adenomas and MSI carcinomas seems to be higher in the proximal than the distal colon, although they are known to occur throughout the large intestine (10, 21). We only examined hyperplastic ACF from the distal colon, and it should be noted that the differences in microenvironment between the ascending and descending colon may ultimately determine whether these lesions progress to more advanced stages of the serrated pathway to colorectal carcinoma (8).

In the alternative pathway encompassing serrated adenomas and carcinomas proposed by Jass et al. (5), *APC* mutations are not determinant, and *BRAF* mutations are prevalent (9, 20). Our finding of a strong association between *BRAF* mutations and serrated histology in hyperplastic ACF supports the idea that these lesions are an early, sentinel, or potentially initiating step on the serrated pathway to colorectal carcinoma.

Acknowledgments

Received 1/30/2007; accepted 3/6/2007.

Grant support: Yellin Golf Foundation, Neag Comprehensive Cancer Center, Jimmy V. Foundation, and NIH grant CA-81428.

The costs of publication of this article were defrayed in part by the payment of page charges. This article must therefore be hereby marked *advertisement* in accordance with 18 U.S.C. Section 1734 solely to indicate this fact.

We thank Olympus for generously providing the endoscopy instrumentation.

References

1. Bird RP. Observation and quantification of aberrant crypts in the murine colon treated with a colon carcinogen: preliminary findings. Cancer Lett 1987;37:147–51.
2. Pretlow TP, Barrow BJ, Ashton WS, et al. Aberrant crypts: putative preneoplastic foci in human colonic mucosa. Cancer Res 1991;51:1564–7.
3. Roncucci L, Stamp D, Medline A, Cullen JB, Bruce WR. Identification and quantification of aberrant crypt foci and microadenomas in the human colon. Hum Pathol 1991;22:287–94.
4. Kinzler KW, Vogelstein B. Lessons from hereditary colorectal cancer. Cell 1996;87:159–70.
5. Jass JR, Whitehall VL, Young J, Leggett BA. Emerging concepts in colorectal neoplasia. Gastroenterology 2002;123:862–76.
6. Torlakovic E, Snover DC. Serrated adenomatous polyposis in humans. Gastroenterology 1996;110:748–55.
7. Hamilton SR. Origin of colorectal cancers in hyperplastic polyps and serrated adenomas: another truism bites the dust. J Natl Cancer Inst 2001;93:1282–3.
8. Yang S, Farraye FA, Mack C, Posnik O, O'Brien MJ. BRAF and KRAS Mutations in hyperplastic polyps and serrated adenomas of the colorectum: relationship to histology and CpG island methylation status. Am J Surg Pathol 2004;28:1452–9.
9. O'Brien MJ, Yang S, Mack C, et al. Comparison of microsatellite instability, CpG island methylation phenotype, BRAF and KRAS status in serrated polyps and traditional adenomas indicates separate pathways to distinct colorectal carcinoma end points. Am J Surg Pathol 2006;30:1491–501.
10. O'Brien MJ, Yang S, Clebanoff JL, et al. Hyperplastic (serrated) polyps of the colorectum: relationship of CpG island methylator phenotype and K-*ras* mutation to location and histologic subtype. Am J Surg Pathol 2004;28:423–34.
11. Torlakovic E, Skovlund E, Snover DC, Torlakovic G, Nesland JM. Morphologic reappraisal of serrated colorectal polyps. Am J Surg Pathol 2003;27:65–81.
12. Greenspan EJ, Cyr JL, Pleau DC, et al. Microsatellite instability in aberrant crypt foci from patients without concurrent colon cancer. Carcinogenesis 2006. Epub Nov 4.
13. Greenspan EJ, Jablonski MA, Rajan TV, et al. Epigenetic alterations in RASSF1A in human aberrant crypt foci. Carcinogenesis 2006;27:1316–22.
14. Yuan P, Sun MH, Zhang JS, Zhu XZ, Shi DR. APC and K-ras gene mutation in aberrant crypt foci of human colon. World J Gastroenterol 2001;7:352–6.
15. Boland CR, Thibodeau SN, Hamilton SR, et al. A National Cancer Institute Workshop on Microsatellite Instability for cancer detection and familial predisposition: development of international criteria for the determination of microsatellite instability in colorectal cancer. Cancer Res 1998;58:5248–57.
16. Goldstein N. Serrated pathway and APC (conventional)-type colorectal polyps. Molecular-morphologic correlations, genetic pathways, and implications for classification. Am J Clin Pathol 2006;125:146–53.
17. Smith G, Carey FA, Beattie J, et al. Mutations in APC, Kirsten-ras, and p53: alternative genetic pathways to colorectal cancer. Proc Natl Acad Sci U S A 2002;99:9433–8.
18. Stevens RG, Swede H, Rosenberg DW. Epidemiology of colonic aberrant crypt foci: review and analysis of existing studies. Cancer Lett. Epub 2006 Dec 18.
19. Beach R, Chan AO, White JA, et al. BRAF mutations in aberrant crypt foci and hyperplastic polyposis. Am J Path 2005;166:1069–75.
20. Chan AO, Broaddus RR, Houlihan PS, Issa JPJ, Hamilton SR, Rashid A. CpG Island Methylation in Aberrant crypt foci of the colorectum. Am J Path 2002;160:1823–30.
21. Spring KJ, Zhao ZZ, Karamatic R, et al. High prevalence of sessile serrated adenomas with BRAF mutations: a prospective study of patients undergoing colonoscopy. Gastroenterology 2006;131:1400–7.

Mutations in *BRAF* and *KRAS* Differentially Distinguish Serrated versus Non-Serrated Hyperplastic Aberrant Crypt Foci in Humans

Daniel W. Rosenberg, Shi Yang, Devon C. Pleau, et al.

Cancer Res 2007;67:3551-3554.